Journal of the Taiwan Institute of Chemical Engineers

Free convection and second law scrutiny of NEPCM suspension inside a wavy-baffle-equipped cylinder under altered Fourier theory

--Manuscript Draft--

Manuscript Number:	JTICE-D-21-00559
Article Type:	SI:Nano-Renewable
Section/Category:	Energy and Environmental Science and Technology
Keywords:	Natural convection; NEPCM, Wavy baffle; Cattaneo-Christov heat flux; Inclined magnetic field; Entropy generation
Corresponding Author:	A. Sattar Dogonchi Babol Noshirvani University of Technology babol, IRAN (ISLAMIC REPUBLIC OF)
First Author:	M.K. Nayak
Order of Authors:	M.K. Nayak
	A. Sattar Dogonchi
	Yasser Elmasry
	Nader Karimi
	Ali J. Chamkha
Abstract:	Background Free convection and second law scrutiny of nano-encapsulated phase change material (NEPCM) suspension along with entropy production inside a circular cold cylinder involving a wavy hot baffle is a significant thermal management aspect subject to various industrial applications. Phase change material (PCM) undergoes a solid-liquid phase mutation at a particular fusion temperature, and absorbs/releases an appreciable amount of energy because of the latent heat of phase mutation. Hence, NEPCMs would be prospective owing to their capability to enhance the working liquids' performance, keeping the system at a particular cooling temperature. Methods In order to simulate the free convection along with entropy generation of NEPCMs inside a circular cold cylinder entails a wavy hot baffle under Cattaneo-Christov heat flux model (Altered Fourier theory) and magnetic field, the finite element method (FEM) could be utilized to solve the governing equations. In this study, the amplitude of baffle could be changeable while its undulation number is fixed at 2. Findings Amplifying Raylegh number intensifies streamlines, isotherms, horizontal and vertical velocities, total entropy generation whittles down local Bejan number. Higher magnetic field strength is responsible for slow movement of NEPCMs and augments local Bejan number. Growth of baffle size yields squeezes the streamlines, horizontal and vertical velocities and intensified tilted isotherms.
Suggested Reviewers:	Abdelraheem M. Aly, PhD King Khalid University ababdallah@kku.edu.sa
	W.A. Khan, PhD Beijing Institute of Technology waqarazeem@bit.edu.cn
	Khalil Ur Rehman, PhD University of Waterloo kurrehman@uwaterloo.ca

Powered by Editorial Manager® and ProduXion Manager® from Aries Systems Corporation

	Muhammad Yousaf Malik, PhD Quaid-i-Azam University drmymalik@qau.edu.pk
	S.M. Seyyedi, PhD Islamic Azad University s.masoud_seyedi@aliabadiau.ac.ir
Opposed Reviewers:	

Powered by Editorial Manager® and ProduXion Manager® from Aries Systems Corporation

COVER LETTER FOR SUBMISSION OF MANUSCRIPT

Subject: **Submission of manuscripts**

Dear Editor,

With this letter, I have attached a copy of manuscript entitled "**Free convection and second law scrutiny of NEPCM suspension inside a wavy-baffle-equipped cylinder under altered Fourier theory**". It is declared that the work described has not been published previously, that it is not under consideration for publication elsewhere, that its publication is approved by all authors and that, if accepted, it will not be published elsewhere in the same form, in English or in any other language, without the written consent of the Publisher.

With best wishes and highest personal regards.

Sincerely yours,

A.S. Dogonchi

Please check the following points before submitting the pdf file for your manuscript. Manuscripts that do not conform may be returned for correction and resubmission. You should be able to answer "yes" to all of the following questions.

- Is the manuscript double-spaced with a font size of 12 pt (Times or Times New Roman preferred)?

  YES

- Have you given full addresses and affiliations for all co-authors?

  YES

- Is the corresponding author identified by an asterisk (*) and their contact details (phone number and e-mail address) given on the first page?

  YES

- Have you given a Graphical Abstract and Highlights of your manuscript?

  YES

- Does the manuscript include a one-paragraph abstract of no more than 200 words for Original Papers or 150 words for Short Communications?

  YES

- Do the length of manuscript and the number of display items obey the requirement?

  YES

- Have keywords (maximum 6) been provided immediately after the abstract?

  YES

- Are sections given Arabic numbers with subsections numbered using the decimal system? NOTE: Acknowledgements and References sections are **not** numbered.

  YES

- Do you embed all figures, tables, and schemes (including the captions) at appropriate places in the text?

  YES

- Are References in the correct format for this journal?

  YES

- Are all references mentioned in the Reference list cited in the text, and vice versa?

YES

- Has the manuscript been spell-checked and grammar-checked?

  YES

- Are all symbols translated correctly in the pdf file?

  YES

- Has written permission been obtained and uploaded as Additional Files for use of copyrighted materials from other sources (including illustrations, tables, text quotations, Web content, etc.)? Has the copyright information been included in the relevant figure caption or table footnote, as an example "Reprinted with permission from Ref. [10]. Copyright 2010 Elsevier"?

  YES

Research Highlights:

- Second law scrutiny of NEPCM suspension inside a circular cylinder is inspected.
- The cold circular cylinder possesses a wavy baffle which acts as a heater.
- The amplitude of hot wavy baffle have a potential to be changed.
- The whole system is assumed to be affected by Cattaneo-Christov heat flux model.
- The governing equations have been solved via the finite element method (FEM).

Manuscript

Click here to view linked References

Free convection and second law scrutiny of NEPCM suspension inside a wavy-baffle-equipped cylinder under altered Fourier theory

M.K. Nayak[1], A. Sattar Dogonchi[2*], Yasser Elmasry[3], Nader Karimi[4], Ali J. Chamkha[5]

[1]Department of Mechanical Engineering, FET, ITER, Siksha 'O' Anusandhan Deemed to be University, Bhubaneswar-751030, India
[2]Independent researcher in Mechanical Engineering
[3]Department of Mathematics, Faculty of Science, Mansoura University, Mansoura 35516, Egypt
[4]School of Engineering and Materials Science, Queen Mary University of London, London E14NS, United Kingdom
[5]Faculty of Engineering, Kuwait College of Science and Technology, Doha District, Kuwait
***Corresponding author:** A. Sattar Dogonchi
(Email address: sattar.dogonchi@yahoo.com, phone number: +989112707743)

ABSTRACT

Background: Free convection and second law scrutiny of nano-encapsulated phase change material (NEPCM) suspension along with entropy production inside a circular cold cylinder involving a wavy hot baffle is a significant thermal management aspect subject to various industrial applications. Phase change material (PCM) undergoes a solid-liquid phase mutation at a particular fusion temperature, and absorbs/releases an appreciable amount of energy because of the latent heat of phase mutation. Hence, NEPCMs would be prospective owing to their capability to enhance the working liquids' performance, keeping the system at a particular cooling temperature.

Methods: In order to simulate the free convection along with entropy generation of NEPCMs inside a circular cold cylinder entails a wavy hot baffle under Cattaneo-Christov heat flux model (Altered Fourier theory) and magnetic field, the finite element method (FEM) could be utilized to solve the governing equations. In this study, the amplitude of baffle could be changeable while its undulation number is fixed at 2.

Findings: Amplifying Raylegh number intensifies streamlines, isotherms, horizontal and vertical velocities, total entropy generation whittles down local Bejan number. Higher magnetic field strength is responsible for slow movement of NEPCMs and augments local Bejan number. Growth of baffle size yields squeezes the streamlines, horizontal and vertical velocities and intensified tilted isotherms.

Keywords: Natural convection; NEPCM, Wavy baffle; Cattaneo-Christov heat flux; Inclined magnetic field; Entropy generation.

1. Introduction

Nano-encapsulated phase change materials (NEPCMs) is a unique type of nanofluid. The nanoparticle of NEPCM comprises of a core and a shell. The core sector may be usually built of phase change material (PCM) that goes through a solid-liquid phase mutation at a particular fusion temperature and during phase change it stores/releases ample energy with aid of the latent heat of phase change (Su et al. [1]). NEPCMs are potentially capable in maintaining the thermal devices at a suitable cooling temperature so as to ameliorate the performance of working fluids. In fact, PCMs and nano-enhanced PCMs find very important usefulness in several engineering aspects include thermal energy storage, thermal management in buildings, heat pump for domestic requirement, air-conditioning, space instruments, cooling in electronic devices, and food processing [2-5]. In order to fulfill the above usefulness, PCMs should have stronger and spawning heat transportation capability. However, PCMs could be intrinsically extremely feeble with reference to heat transfer. In view of enhancing heat transfer features of PCM, many researchers have endeavored to accomplish this through their research by considering fins, porous media, nanoparticles as Nano-Enhanced Phase Change Materials (NEPCMs) and Nano-Encapsulated Phase Change Materials (NEPCMs). In former the solid nano-materials could be usually added to PCM to augment heat transmission properties whereas in latter the PCMs could be basically encapsulated inside a capsule shell of nanometer-size, and then these developed materials could be diffused within a working liquid (Sheikholeslami [5], Hossain et al. [6], Ghalambaz et al. [7], Hosseini et al. [8], Sheikholeslami and Sadoughi [9], Elbahjaoui and Qarnia [10]).

The mechanism of natural convection (NC) in a cavity finds enormous applications in heat exchangers, solar collecting devices, ducts, reactors (chemical and nuclear), cooling of electronic devices, and many. The investigations of NC in an area among concentric circular and square cylinders (Moukalled and Acharya [11]), space between heated cylindrical element

and its rectangular enclosure (Ghaddar [12]), space surrounding a square, heated cylinder placed inside an enclosure (Kumar and Dalal [13]), square enclosure containing a circular cylinder at several vertical locations (Kim et al. [14]), square enclosure (Yoon et al. [15]), and square enclosure possessing circular cylinder at various horizontal and diagonal positions (Lee et al. [16]) were carried on effectively. Recently, Li et al. [17] inspected the influence of NC and entropy generation around a roundish baffle enshrined in an inclined square enclosure. They also analyzed the effect of thermal radiation and magnetic field in the system. Entropy generation conveys the information regarding the energy efficiencies of thermo fluidics systems for several nanofluids [18, 19]. A review on entropy generation associated with natural convection heat transfer for various energy systems was presented by Oztop and Al-Salem [20]. Oztop et al. [21] carried out a three dimensional approach on entropy generation by buoyancy driven flow and HT in partially open cavity. Further, Selimefendigil et al. [22] explored entropy generation effect of nanoliquid inside a lid-driven enclosure under the influence of uniform inclined magnetic fields. It was observed that the local and mean HT peters out due to the amplification of Richardson number and Hartmann number. Heat transfer mechanism contributes a significant role in their extensive uses in diversified engineering/industrial systems such as atomic controller refrigeration, biomedicine, heat exchange, liquid distillation, nuclear reactor cooling, solar system technology, space cooling, energy production, heat conduction in tissues and many others. Starting from Fourier [23] ending at Christov [24] via Cattaneo [25] developed mechanism/modeling led to the description of better HT characteristics. Later, flow and HT behavior were presented through the investigations in the influence of CCHFM on the flow of burgers fluid (Waqas et al. [26]), improved Fourier's and Fick's laws applied to a non-Newtonian fluid (Waqas et al. [27]) and radiative MHD squeezed flow of nanofluid (Dogonchi and Ganji [28]).

MHD flows coupled with natural convection is very demanding one because of its practical and inevitable applications/occurrences in crystal growing, cooling of electronic/ microelectronic devices and nuclear reactors, thermal insulation, solar collectors, manufacturing of semiconductors etc.. In addition, effect of orientation of magnetic field would be highly significant to administer HT, fluid flow, energy efficiency and temperature distribution. Many researchers have implanted their mind in investigating MHD natural convection impact on flow and HT in enclosures of different shapes associated with different conditionalties. For example, MHD natural convection influence and HT aspect in nf flow through permeable cavity (Sheikholeslami et al. [29]), flow of electrically conducting liquid gallium inside a cavity subject inclined magnetic field and with uniformly heated wall, linearly heated the left and right vertical walls and thermally insulated top wall (Sathiyamoorthy and Chamkha [30]), in an enclosure having sidewalls featured with sinusoidal boundary temperatures (Sivasankaran et al. [31]), flow inside a top sided lid-driven enclosure heated by a corner heater where HT whittles down with amplifying Hartmann number (Oztop et al. [32]), nf flow in a horizontal cylindrical annulus enclosure (Ashorynejad et al. [33]), phase alteration material in the existence of magnetic field (Ghalambaz et al. [34]), nanoliquid flow in horizontal partitioned annulus subject to an inclined magnetic field (Selimefendigil and Oztop [35]). Recently, the impact of magnetic field employed from either the warmed wall's left bottommost corner or the cool wall's right bottommost corner on NC inside a cavity was explored by Geridonmez and Oztop [36]. In their study, the effect of magnetic field’s angle on vorticity, isotherms, and streamlines contours as well as mean Nu through the warmed wall was explored. Further, NC and EG of a nf surrounding a circular baffle contained in an inclined square cavity under the impact of magnetic field was analyzed by Li et al. [37]. According to their results amplifying Ra augmented the Nu by 4.5 times and grows EG, however, peters out Bejan number. The HTR and EG get upsurged with amplification of aspect ratio.

Derived from authors' knowledge and above literature overview it is visualized that due to difficult meshing there is no study on wavy baffle inside a circular cylinder filled with NEPCMs in earlier works. This type of work involving PCMs has immense potential due to its applications in science, engineering and modern industries. Therefore, the present study is very much important to understand the influence of free convection of NEPCMs inside a circular cold cylinder entailing a wavy hot baffle of varying amplitude subject to inclined magnetic field and CCHFM. The problem is modeled in the form of dimensionless governing equations with aid of nondimensionalized variables. The numerical simulations are accomplished by finite element method. The influence of Hartmann and Rayleigh numbers, direction of applied magnetic field, size of wavy baffle, fusion temperature on the isotherms, streamlines, heat capacity ratio, dimensionless horizontal and vertical velocities, local and average Nusselt numbers and local Bejan number along the wavy hot baffle is examined numerically on HT and flow of NEPCMs in circular cold cylinder. The results are presented in the form of apposite diagrams and tables.

2. Governing Equations

This part represents the governing equations of free convection of Nano-Encapsulated Phase Change Materials (NEPCMs) inside a circular cold cylinder entails a wavy hot baffle. The amplitude of this baffle may be changeable while its undulation number is fixed at 2. The whole system is supposed to be affected by magnetic field and Cattaneo-Christov heat flux model and the fluid flow inside is considered to be incompressible, laminar, steady, and two-dimensional. Based on these facts as well as Boussinesq viewpoint we could express the governing equations as:

$$\frac{\partial u}{\partial x}+\frac{\partial v}{\partial y}=0 \tag{1}$$

$$\rho_b\left(u\frac{\partial u}{\partial x}+v\frac{\partial u}{\partial y}\right)=-\frac{\partial p}{\partial x}+\mu_b\left(\frac{\partial^2 u}{\partial x^2}+\frac{\partial^2 u}{\partial y^2}\right)+B_0^2\delta_b\begin{pmatrix}\cos(\Upsilon)\sin(\Upsilon)v\\-\sin(\Upsilon)\sin(\Upsilon)u\end{pmatrix} \tag{2}$$

$$\rho_b\left(u\frac{\partial v}{\partial x}+v\frac{\partial v}{\partial y}\right)=-\frac{\partial p}{\partial y}+\mu_b\left(\frac{\partial^2 v}{\partial x^2}+\frac{\partial^2 v}{\partial y^2}\right)+B_0^2\delta_b\begin{pmatrix}\cos(\Upsilon)\sin(\Upsilon)u\\-\cos(\Upsilon)\cos(\Upsilon)v\end{pmatrix}+\rho_b\beta_b g\left(T-T_c\right) \tag{3}$$

$$\left(\rho C_p\right)_b\left(u\frac{\partial T}{\partial x}+v\frac{\partial T}{\partial y}\right)=-\nabla.\mathbf{q}, \tag{4}$$

in which **q** could be exhibited as:

$$\mathbf{q}+\gamma\left((\nabla.\mathbf{V})\mathbf{q}+\mathbf{V}.\nabla\mathbf{q}-\mathbf{q}.\nabla\mathbf{V}\right)=-k_b\nabla T\,. \tag{5}$$

by eradicating the **q** from the last two equations, one could obtain:

$$\left(u\frac{\partial T}{\partial x}+v\frac{\partial T}{\partial y}\right)+\gamma\begin{pmatrix}2uv\dfrac{\partial^2 T}{\partial x\,\partial y}+u\dfrac{\partial u}{\partial x}\dfrac{\partial T}{\partial x}+\\ v\dfrac{\partial v}{\partial y}\dfrac{\partial T}{\partial y}+v\dfrac{\partial u}{\partial y}\dfrac{\partial T}{\partial x}+\\ v^2\dfrac{\partial^2 T}{\partial y^2}+u^2\dfrac{\partial^2 T}{\partial x^2}+u\dfrac{\partial v}{\partial x}\dfrac{\partial T}{\partial y}\end{pmatrix}=\frac{k_b}{\left(\rho C_p\right)_b}\left(\frac{\partial^2 T}{\partial x^2}+\frac{\partial^2 T}{\partial y^2}\right), \tag{6}$$

To solve these governing equations, one should convert them to their non-dimensional format with the aid of the below parameters:

$$\begin{aligned}&X=\frac{x}{L},\quad U=\frac{uL}{\alpha_f},\quad \theta=\frac{T-T_c}{T_h-T_c},\qquad V=\frac{vL}{\alpha_f},\qquad Y=\frac{y}{L},\quad P=\frac{pL^2}{\rho_f\alpha_f^2}\\&\rho_b/\rho_f=\phi\left(\rho_p/\rho_f\right)+(1-\phi),\qquad \beta_b/\beta_f=\phi\left(\beta_p/\beta_f\right)+(1-\phi)\\&\mu_b/\mu_f=(1+N_v\phi),\qquad \delta_b/\delta_f=(1+N_e\phi),\qquad k_b/k_f=(1+N_c\phi)\end{aligned} \tag{7}$$

therefore, dimensionless format of governing equations would be as:

$$\left(U\frac{\partial U}{\partial X}+V\frac{\partial U}{\partial Y}\right)=-\frac{1}{\phi\left(\rho_p/\rho_f\right)+\left(1-\phi\right)}\frac{\partial P}{\partial X}+\frac{\left(1+N_v\phi\right)}{\phi\left(\rho_p/\rho_f\right)+\left(1-\phi\right)}\Pr\left(\frac{\partial^2 U}{\partial X^2}+\frac{\partial^2 U}{\partial Y^2}\right)+\frac{\left(1+N_e\phi\right)}{\phi\left(\rho_p/\rho_f\right)+\left(1-\phi\right)}\Pr Ha^2\begin{pmatrix}\cos(\Upsilon)\sin(\Upsilon)V\\-\sin(\Upsilon)\sin(\Upsilon)U\end{pmatrix} \tag{8}$$

$$\left(U\frac{\partial V}{\partial X}+V\frac{\partial V}{\partial Y}\right)=-\frac{1}{\phi\left(\rho_p/\rho_f\right)+\left(1-\phi\right)}\frac{\partial P}{\partial Y}+\frac{\left(1+N_v\phi\right)}{\phi\left(\rho_p/\rho_f\right)+\left(1-\phi\right)}\Pr\left(\frac{\partial^2 V}{\partial X^2}+\frac{\partial^2 V}{\partial Y^2}\right)+\frac{\left(1+N_e\phi\right)}{\phi\left(\rho_p/\rho_f\right)+\left(1-\phi\right)}\Pr Ha^2\begin{pmatrix}\cos(\Upsilon)\sin(\Upsilon)U\\-\cos(\Upsilon)\cos(\Upsilon)V\end{pmatrix}+\left[\phi\left(\beta_p/\beta_f\right)+\left(1-\phi\right)\right]Ra\Pr\theta \tag{9}$$

$$\left(U\frac{\partial\theta}{\partial X}+V\frac{\partial\theta}{\partial Y}\right)+\eta\begin{pmatrix}2UV\dfrac{\partial^2\theta}{\partial X\,\partial Y}+U\dfrac{\partial U}{\partial X}\dfrac{\partial\theta}{\partial X}\\+V\dfrac{\partial V}{\partial Y}\dfrac{\partial\theta}{\partial Y}+V\dfrac{\partial U}{\partial Y}\dfrac{\partial\theta}{\partial X}\\+U^2\dfrac{\partial^2\theta}{\partial X^2}+V^2\dfrac{\partial^2\theta}{\partial Y^2}\\+U\dfrac{\partial V}{\partial X}\dfrac{\partial\theta}{\partial Y}\end{pmatrix}=\frac{\left(1+N_c\phi\right)}{\left(\rho C_p\right)_b/\left(\rho C_p\right)_f}\left(\frac{\partial^2\theta}{\partial X^2}+\frac{\partial^2\theta}{\partial Y^2}\right) \tag{10}$$

where N_e and N_v indicate the numbers of electrical conductivity and dynamic viscosity and the ratio of $\left(\rho C_p\right)_b$ to $\left(\rho C_p\right)_f$ may well be defined as *Cr* which is the heat capacity ratio and could be demonstrated as [38]:

$$C_r=\frac{\phi}{\chi Ste}f+\left(1-\phi\right)+\phi\lambda \tag{11}$$

in which *Ste* and *f* indicate the Stefan number and the dimensionless fusion function, respectively and the f could be expressed as:

$$f = \frac{\pi}{2}\sin\left(\frac{\pi}{\Gamma}\left(\theta-\theta_f+\frac{\Gamma}{2}\right)\right)\times\begin{cases}0 & \theta<\theta_f-\dfrac{\Gamma}{2}\\ 1 & \theta_f-\dfrac{\Gamma}{2}<\theta<\theta_f+\dfrac{\Gamma}{2}\\ 0 & \theta>\theta_f+\dfrac{\Gamma}{2}\end{cases} \tag{12}$$

here θ_f is the dimensionless fusion temperature.

For the current work the boundary conditions could be expressed as:

$$\begin{array}{llll}\Psi=0 & \text{on all walls} & \theta=1 & \text{on the baffle}\\ & \theta=0 & \text{on the cylinder} & \end{array} \tag{13}$$

and the local and mean Nusselt number on the cold cylinder may be demonstrated as:

$$Nu_{loc.}=-\left(1+N_c\phi\right)\frac{\partial\theta}{\partial n},\ Nu_{ave.}=\frac{1}{2\pi}\int_0^{\xi}Nu_{loc.}d\xi \tag{14}$$

In this paper we also analyse the entropy generation (En) which may be expressed as:

$$\begin{aligned}En_{local}=&\left(1+N_e\phi\right)\Lambda Ha^2\begin{pmatrix}U\sin(\Upsilon)\\ -V\cos(\Upsilon)\end{pmatrix}^2+\left(1+N_v\phi\right)\Lambda\left[2\left(\frac{\partial U}{\partial Y}\right)^2+2\left(\frac{\partial U}{\partial X}\right)^2+\left(\frac{\partial U}{\partial X}+\frac{\partial U}{\partial Y}\right)^2\right]\\ &+\left(1+N_c\phi\right)\left[\left(\frac{\partial\theta}{\partial Y}\right)^2+\left(\frac{\partial\theta}{\partial X}\right)^2\right]\end{aligned} \tag{15}$$

where the first, second and third terms demonstrate the local entropy generation owing to magnetic field ($En_{local,\ MF}$), fluid friction ($En_{local,\ FF}$), and heat transfer ($En_{local,\ HT}$), respectively and the local entropy generation (En_{local}) might well be the summation of these terms. The integration of En_{local} could result in the total entropy generation as:

$$En_{total}=\int_V En_{local}\,\mathrm{dV}. \tag{16}$$

And finally the local or mean Bejan number could be characterized as:

$$\begin{aligned}Be_{local}&=\frac{En_{local,HT}}{En_{local}}\\ Be_{ave.}&=\frac{\int_A Be_{local}\,\mathrm{dA}}{\int_A \mathrm{dA}}\end{aligned} \tag{17}$$

3. Numerical method and validation

In this paper, we apply the FEM to obtain an accurate solution for the current problem. Moreover, a comparison with other works [39,40] has been done to ascertain the validity of this method. This comparison which is portrayed in figure 2 displays a plausible agreement with the outcomes of [39] and [40].

4. Results and discussion

This segment conveys the interpretation of CFD results of the modelling enshrining the aspect of free convection and second law of NEPCM suspension inside a circular cold cylinder involving a wavy hot baffle. Finite element method is the instrumental of accomplishing the complete numerical solution of the non-dimensional governing equations of the present problem. The influence of relevant embedded parameters such as Hartmann number (Ha), the amplitude of wavy baffle (b), dimensionless fusion temperature (θ_f), Rayleigh number (Ra), the volume fraction of nanoliquid (ϕ), and thermal relaxation parameter (η) on stream functions, isotherms, heat capacity ratio, horizontal and vertical velocities, local Bejan number, Local and average Nusselt numbers, and total entropy generation in association with the magnetic free convection of NEPCMs within a circular cold cylinder embodies a wavy hot baffle is dissected. In the beginning of the discussion, it starts with Fig.3 that explains the behavior of isotherms (left), streamlines (middle) and heat capacity ratio (Cr) contours for varied estimations of Ha and Ra when $N = 2, \phi = 0.05, Ste = 0.2, b = 0.1$ and $\theta_f = 0.35$ .In the absence of magnetic field $(Ha = 0)$, streamlines get intensified due to uplift in Rayleigh number (Ra). In fact, $|\Psi|_{\max}$ corresponding to natural convection's intensity depends on Ra. This implicates that the natural convection characteristics of nano encapsulated phase change materials (NEPCMs) follow a positive correlation with Ra .Because of this fluid runs faster on

both sides of hot wavy baffle within the cylinder. As observed in Fig. 3, for Ha=0, $\left|\Psi_{\max}\right|^{Ra=10^3} = 0.158142 > \left|\Psi_{\max}\right|^{Ra=10^4} = 1.58191 > \left|\Psi_{\max}\right|^{Ra=10^5} = 7.50013$. This means that when Ra amplifies, the buoyancy force inside the system upgrades which in turn intensifies the intensity of NC of NEPCMs there by causes the fast movement of the fluid within the cylinder. In order to administrate the NC, a magnetic field is imposed to the system. Magnetic field possesses a direct correlation with the power of NC of NEPCMs. Therefore, applied magnetic field $(Ha \neq 0)$ yields a sluggish movement of fluid within the cylinder keeping the wavy baffle intact in its position. Referring to Fig.3, its evidence is obtained as $\left|\Psi_{\max}\right|^{Ha=0} = 1.58191 > \left|\Psi_{\max}\right|^{Ha=10} = 1.16258 > \left|\Psi_{\max}\right|^{Ha=20} = 0.657064$ for $Ra = 10^4$. Similar correlation is seen for $Ra = 10^3$ and $Ra = 10^5$. It conveys us that a magnetic field can be served as a controlling element for the fluid flow process. In the absence/presence of magnetic field, two vertices are produced in the cavity on both sides of the wavy hot baffle (WHB) at low and high Raleigh numbers. The formation of vertices is due to the density difference inside the cylinder which is due to the difference in nanofluid near constant temperature walls and baffle. As far as isotherm contours are concerned, isotherms contiguous to wavy baffle exhibit wavy shape isotherms irrespective of the value of Ra. This is due to the heat conduction from the wavy shaped baffle. In addition, for low Ra (for instance $Ra = 10^3$), symmetric ordered elliptical contours (isotherms) appear surrounding the WHB. This is because of weak buoyancy force due to low value of Ra. When Ra amplifies, the buoyancy force upgrades which in turn yields more symmetric isotherms of disorderly shape around the centrally situated WHB of fixed amplitude $(b = 0.1)$. Cr in Fig. 3 portrays elliptical ring form around the fusion region for low Ra while it shows a disordered shape at high Ra. The Cr outside the fusion region and wavy baffle attains a constant value 0.97 and varies inside the fusion temperature irrespective of the values of Ra. The red part created in Cr contours of Fig. 3 represents the phase change

section. The ring shape of the phase mutation area is very thin due to uniform and large temperature gradients. In Fig. 3, at each value of Ra, fusion region surrounds the wavy baffle. The change in fusion temperature affects the streamlines significantly. Fig. 4 demonstrates the horizontal and vertical velocities respectively U and V for different values of Ra with or without magnetic field. Without influence of magnetic field $(Ha = 0)$, U and V amplify with rise in Ra i.e., $|U_{\max}|^{Ra=10^3} = 0.58527 < |U_{\max}|^{Ra=10^4} = 6.23046 < |U_{\max}|^{Ra=10^5} = 34.4471$ and $|V_{\max}|^{Ra=10^3} = 1.15298 < |V_{\max}|^{Ra=10^4} = 11.8068 < |V_{\max}|^{Ra=10^5} = 59.9716$. More elaborately it is observed that with $Ha = 0$ at $Ra = 10^3, 10^4, 10^5$ four vertices are formed (two at upper part and two at lower part of the cavity). In addition, some less intensified vertices (due to less buoyancy as a result of low Ra) are appeared at the top and bottom of the cylinder. At two diagonally opposite vertices U contours decline for each chosen value of Ra. Further, V contours appear in the form of irregular shapes with vertices on opposite sides of HWB and also at upper and lower portions of the cavity for $Ra = 10^3, 10^4, 10^5$. However, with the magnetic field $(Ha \neq 0)$, the vertices whittle down with irrespective values of Ra. For example, at fixed Ra ($Ra=10^4$) rise in Ha peters out U and V. More evidently, $|U_{\max}|^{Ha=0} = 6.23046 > |U_{\max}|^{Ha=10} = 4.57964 > |U_{\max}|^{Ha=20} = 2.69129$ and $|V_{\max}|^{Ha=0} = 11.8068 > |V_{\max}|^{Ha=10} = 8.76297 > |V_{\max}|^{Ha=20} = 5.1805$ for $Ra = 10^4$. In this case as the value of Ra goes on increasing, U and V upsurge due to increase in natural convective forces gained by NEPCMs at fixed value of other parameters. In other words, an uplift in Ra from 10^3 to 10^4 or 10^4 to 10^5, the thermal gradient enhances and this enhancement in thermal gradient causes an augmentation in the value of velocity gradient. Consequently U and V get upsurged. At extreme Ra, fluid takes away more heat from the WHB and it transports to the cold walls of the cylinder and therefore more noteworthy heat exchange among HWB, NEPCM

(fluid) and cold side walls of the cylinder. As a result, this greater temperature difference leads to more buoyancy causing a notable improvement in U and V. Further, in Fig. 4 it is ensured that rise in magnetic field weakens the buoyancy force thereby diminishing U and V. Fig. 5 narrates the θ, Ψ and Cr for different angle of inclination γ at diverse Ra $\left(Ra = 10^3, 10^4, 10^5\right)$ with fixed N=2, ϕ=0.05, Ste=0.2, b=0.1, Ha=20, and θ_f=0.35. For $\gamma = 0$ (with no inclination of magnetic field), rise in Ra ensures the augmentation of streamline contours (due to the enhancement of buoyancy force). At fixed Ra (for instance $Ra = 10^4$), increase in γ $\left(\gamma = 0^0, 30^0, 60^0, 90^0\right)$ upgrades the stream functions marginally. Evidently $\left|\Psi_{\max}\right|^{\gamma=0^0} = 0.0663896 < \left|\Psi_{\max}\right|^{\gamma=30^0} = 0.0754844 < \left|\Psi_{\max}\right|^{\gamma=60^0} = 0.0968891 < \left|\Psi_{\max}\right|^{\gamma=90^0} = 0.112303$. However, this upgradation is prominent at higher value of Ra (for instance $Ra = 10^5$). Evidently, $\left|\Psi_{\max}\right|^{\gamma=0^0} = 4.58131 < \left|\Psi_{\max}\right|^{\gamma=30^0} = 4.781 < \left|\Psi_{\max}\right|^{\gamma=60^0} = 6.10325 < \left|\Psi_{\max}\right|^{\gamma=90^0} = 6.57722$. At each value of Ra with $\gamma = 0^0$ or $\gamma \neq 0^0$, two vertices (one at the front side and the other at the back side of the WHB) are formed. At fixed γ, streamlined contours get intensified due to amplifying Ra. In fact, rise in Ra causes more circulation of NEPCM particles under natural convection within the cylinder. Further, increment in γ yields amplification of isotherms at each fixed Ra. However, at fixed γ (for instance $\gamma = 30^0$), rise in Ra contributes to the greater intensification of isotherms. In fact, PCM cores go through phase mutation from solid to liquid and receive part of surrounding's heat (due to conduction from WHB) in form of latent heat inside the hot area and then released the received heat inside the cold area contiguous to cylinder wall by solidification. In Fig. 5 it is visualized that amplified γ does not contribute any significant variations in Cr at fixed Ra. However, at fixed γ, rise in Ra augments the phase change region in the Cr contours. Meanwhile, the shape of Cr contours changes from $Ra = 10^3$ to $Ra = 10^4$ and from $Ra = 10^4$ to $Ra = 10^5$ (contours of regular and irregular shapes symmetric with respect

to WHB). It is interesting to mention here that Cr value attains a constant value (0.97) outside the fusion region with irrespective values of γ and Ra. Fig. 6 delineates the variations of horizontal and vertical velocities U and V respectively for varied γ at N=2, ϕ=0.05, Ste=0.2, b=0.1, Ha=20, and θ_f=0.35. From this figure it is visualized that at fixed γ (for example at $\gamma = 30^0$), increase in Ra contributes to escalation of U and V. When Ra rises from $Ra = 10^3$ to $Ra = 10^4$, U and V get moderate upgradation due to moderate buoyancy force. Evidently, for $\gamma = 30^0$, $|U_{\max}|$ rises from 0.257679 to 2.69129 and $|V_{\max}|$ rises from 0.520239 to 5.1805. Further, when Ra rises from $Ra = 10^4$ to $Ra = 10^5$, U and V exhibit tremendous upgradation due to large buoyancy force. Evidently, for $\gamma = 30^0$, $|U_{\max}|$ rises from 2.69129 to 21.7731 and $|V_{\max}|$ rises from 5.1805to 37.966. It is interesting to explore that the pattern of U field lines is totally different from that of V field lines at each value of Ra. Specifically, U velocity pattern comprises of four vortices at four diagonally opposite corners within the cavity along with six small vertices on both sides of WHB. Further, V velocity pattern comprises of two vortices on diametrically opposite sides within the cavity along with symmetric V contours with four vortices on opposite sides of WHB. At fixed Ra (for instance $Ra = 10^3$), when γ takes higher values, U and V get intensified, but marginally at low Ra and significantly at high Ra. Fig. 7 conveys the variations of the θ, Ψ and Cr for different b (size of the baffle) and Ra at fixed N=2, ϕ=0.05, Ste=0.2, b=0.1, Ha=20, and θ_f=0.35. The first row of Fig. 7 indicates θ, Ψ, and Cr variations for straight baffle ($b = 0$) for different Ra. For straight baffle case, increase in Ra intensifies streamline contours (streamlines become more dense). Evidently, $|\Psi_{\max}|^{Ra=10^3} = 0.202983 < |\Psi_{\max}|^{Ra=10^4} = 1.86052 < |\Psi_{\max}|^{Ra=10^5} = 8.34528$ for $b = 0$. For each value of Ra, symmetric streamline contours comprising two vortices on either side of straight baffle are accomplished. As far as isotherm variations are concerned, symmetric vertically

elliptical contours surrounding the straight baffle for $Ra = 10^3$ either side are obtained. As Ra amplifies more intensified symmetric contours get created. In addition, amplifying Ra makes Cr intensification for the baffle with $b = 0$. When baffle size amplifies (corresponding to second, third and fourth row) streamline contour diminishes. Evidently,

$\left|\Psi_{\max}\right|^{b=0} = 0.202983 < \left|\Psi_{\max}\right|^{b=0.1} = 0.158142 < \left|\Psi_{\max}\right|^{b=0.2} = 0.124947$ for $Ra = 10^3$. Due to increase in size of wavy baffle, space between WHB and cold wall reduces thereby decreasing the buoyancy leading to diminishing streamline contours. As baffle size grows, conductive HTR augments due to the diminution of the distance between the hot baffle and the cold wall of the cylinder (here conductive HT mechanism is the dominating process). However, at high Rayleigh number, amplification of baffle size augments the HTR due to the dominance of convective HT mechanism via NEPCM. In this case, the change of Ra changes the patterns of isotherms significantly. Further, the change of baffle size yields inclined patterns of isotherms. Fig. 8 reveals the fact of U and V variations for both straight baffle ($b = 0$) and wavy baffle ($b \neq 0$) for varied Ra ($Ra = 10^3, 10^4, 10^5$) at fixed N=2, ϕ=0.05, Ste=0.2, Ha=0 and θ_f=0.35. Irrespective of baffle size (straight or wavy), amplification of Ra intensifies U and V significantly. In case of straight baffle, U contours comprise of four vortices. More elaborately, two vortices are created at diametrically opposite sides and contiguous to the cold wall of the cylinder due to convection dominance between NEPCM and cold wall. Further, two vortices are created on both sides of baffle due to conduction dominance between hot baffle and NEPCM. Further, as baffle size grows, the shape for vortex formation reduces which in turn whittles down U and V inside the cylinder. Evidently,

$\left|U_{\max}\right|^{b=0} = 0.732338 < \left|U_{\max}\right|^{b=0.1} = 0.58527 < \left|U_{\max}\right|^{b=0.2} = 0.491768 < \left|U_{\max}\right|^{b=0.3} = 0.431582$

and $|V_{\max}|^{b=0} = 1.34849 < |V_{\max}|^{b=0.1} = 1.15298 < |V_{\max}|^{b=0.2} = 1.03337 < |V_{\max}|^{b=0.3} = 0.847537$ for $Ra = 10^3$. Fig. 9 indicates the variation of Cr for diverse θ_f and Ra at fixed N=2, ϕ=0.05, Ste=0.2, Ha=0, and θ_f=0.35. At $Ra = 10^3$ and θ_f=0.05, the Cr inside the fusion region (circular red ring) is constant as 0.97. Further, Cr attains the same value but with slightly rise in fusion region when Ra amplifies from $Ra = 10^3$ to $Ra = 10^4$. At θ_f=0.05, when Ra amplifies from $Ra = 10^4$ to $Ra = 10^5$, Cr value remains the same inside the fusion region. However, a wider fusion region of different shape is appeared. When θ_f changes from θ_f=0.05 to θ_f=0.35, Cr attains the constant value as 0.97 outside the thin fusion region of diminishing shape sorrounding the WHB at each chosen value of Ra. With further increase of θ_f (θ_f=0.35 to θ_f=0.65), Cr attains the same constant value outside the further squeezed fusion region sorrounding the WHB with irrespective the value of Ra.At large θ_f (θ_f=0.95), Cr attains constant value as 0.97 outside the thicker fusion region (phase change area) of wavy shape similar to the shape of wavy baffle. Fig. 10 delineates the behavior of local Bejan number (Be_{local}) for different Ra ($Ra = 10^3, 10^4$) for both straight and wavy baffles with or without magnetic field. The Bejan number measures the contribution of thermal entropy to the total EG. At fixed Ra (for instance $Ra = 10^3$), Be_{local} gradually diminishes as we approach we approach towards cold wall of the cylinder from WHB. When Ra amplifies Be_{local} peters out without magnetic field ($Ha = 0$) or with magnetic field ($Ha \neq 0$) for straight baffle ($b = 0$) as well as wavy baffle ($b \neq 0$). This is due to the fact that the velocity gradient significantly augments due to growth of Ra. Temperature gradient also gets amplified. Further, at fixed Ra (for instance at $Ra = 10^3$), Be_{local} intensifies due to amplifying Ha for both straight baffle ($b = 0$) and wavy baffle ($b \neq 0$). Further, at fixed Ra (for instance at $Ra = 10^3$), Be_{local} upsurges for wavy baffle ($b = 0.1, 0.2, 0.3$) compared to straight baffle (b=0) with or without magnetic field.

Specifically, intensified Be_{local} is attained inside the domain of WHB under the influence of magnetic field and also at higher Ra even in the absence of magnetic field. Fig. 11 demonstrates the local Nusselt number (Nu_{local}) variation for different Ra $\left(Ra = 10^3, 10^4\right)$ for straight and wavy baffles with or without magnetic field. Fig. 11(a) illustrates Nu_{local} variation for different b (b=0, 0.1, 0.2, 0.3) for $Ra = 10^3$ in the absence of magnetic field (Ha=0). It is found that at lower and higher ζ , Nu_{local} variation is marginal indicating the dominance of convective HTR over conductive HTR. Same marginal variations are the results for $\zeta = 192^\circ$. At other values of ζ , Nu_{local} amplifies due to rise in b. In fact, amplifying b yields a diminution of temperature gradient. The wave nature of Nu_{local} is due to the wave shape of the baffle. Fig. 11(b) represents Nu_{local} for $Ra = 10^4$ with Ha=0 for both straight and wavy baffles. For ζ $\left(90^\circ \le \zeta \le 270^\circ\right)$, Nu_{local} variation is prominent indicating the dominance of conductive HTR. On the comparison of Fig. 11 (a) and Fig. 11 (b) it is clear that Nu_{local} has greater magnitude for each b value. Fig. 11 (c) and 11 (d) reveal the variation of different b in the presence of magnetic field (Ha=20) for $Ra = 10^3$ and $Ra = 10^4$ respectively. It is understood that Nu_{local} variation is prominent under the influence of Lorentz force due to the applied magnetic field. The generated Lorentz force peters out the temperature gradient and therefore whittles down the HTR (preferably at higher Ra). ig. 12 illustrates Nu_{ave} and En_{total} for varied Ha and Ra against the size of the wavy baffle. As the baffle size amplifies, Nu_{ave} upsurges with or without magnetic field. When baffle size increases, the NEPCM would receive more heat and hence release more heat to the space between solified NEPCM and cold wall of the cylinder. This leads to the augmentation of temperature gradient and therefore amplification of the HTR. Further, HTR amplifies significantly due to augmentation of Ra at lower size of baffle (conductive HTR amplifies) without magnetic field (Ha=0). However, HTR amplification is marginal at higher Ra at higher

baffle size (convective HTR amplifis) under the influence of magnetic field (Ha=20). Total EG amplifies with amplifying baffle size. This is because of large velocity of vortices with larger wavy baffles. Further, amplifying Ra causes an augmentation in both temperature and velocity gradients leading to intensification of En_{total}. En_{total} variation due to Ra change is prominent at low baffle size and is marginal at higher baffle size. However, the overall En_{total} attains slight increase with Ra amplification against b in the existence of magnetic field (Ha=20). Table 1 enlists the Nu_{ave} for different Ra, Ha, and ϕ. It is clear that Nu_{ave} intensifies due to amplification of Ra with Ha=0 or Ha=20. Intensifying Ha causes diminution of Nu_{ave} at $Ra = 10^4$ and $Ra = 10^5$. Further, Nu_{ave} grows due to rise in ϕ in the absence or presence of magnetic field. Table 2 incorporates the numerical alue of Nu_{ave} for different η and Ra. It is obvious that Nu_{ave} belittles due to growth in η for $Ra = 10^3$ and $Ra = 10^4$. Further, amplification in Ra leads to reduction in Nu_{ave} for positive η.

Conclusions

Free convection HT in NEPCMs inside a circular cold cylinder entailing a wavy hot baffle of varying amplitude subject to magnetic field and CCHF is analyzed. The results from investigating the effects of several parameters are briefed as:

- Amplifying Ra accounts for fast movement of fluid while that of Ha causes slow movement of fluid depending upon the intensity of natural convection of NEPCMs.
- Isotherms get intensified due to rise in Ra.
- U and V amplify with hike in Ra and ζ. The structure of U and V contours are entirely different from each other.
- Augmented γ ensures enhancement of stream functions as well as isotherms.

- Shape of Cr contours change with change of Ra. At low Ra and θ_f, Cr attains a constant value as 0.97 inside the fusion region while at higher Ra and θ_f, Cr attains that constant value along with the change of shape of the fusion region.
- Growing baffle size leads to diminution of streamlines, U and V while that of baffle size yields tilted and intensified isotherms depending on the value of RA.
- Be_{local} whittles down with amplifying Ra while that intensifies due to rise in Ha irrespective the nature of the baffle (straight or wavy).
- Nu_{local} escalates due to rise in baffle size while it reduces with rise in Ha against ζ.
- HTR intensifies significantly due to rise in Ra at low b while that is marginal at high Ra and b.
- Total EG upsurges with amplifying Ra leading to prominent augmentation at low b and marginal enhancement at high b (with or without Ha).
- HTR grows with rise in ϕ while that declines due to rise in η.

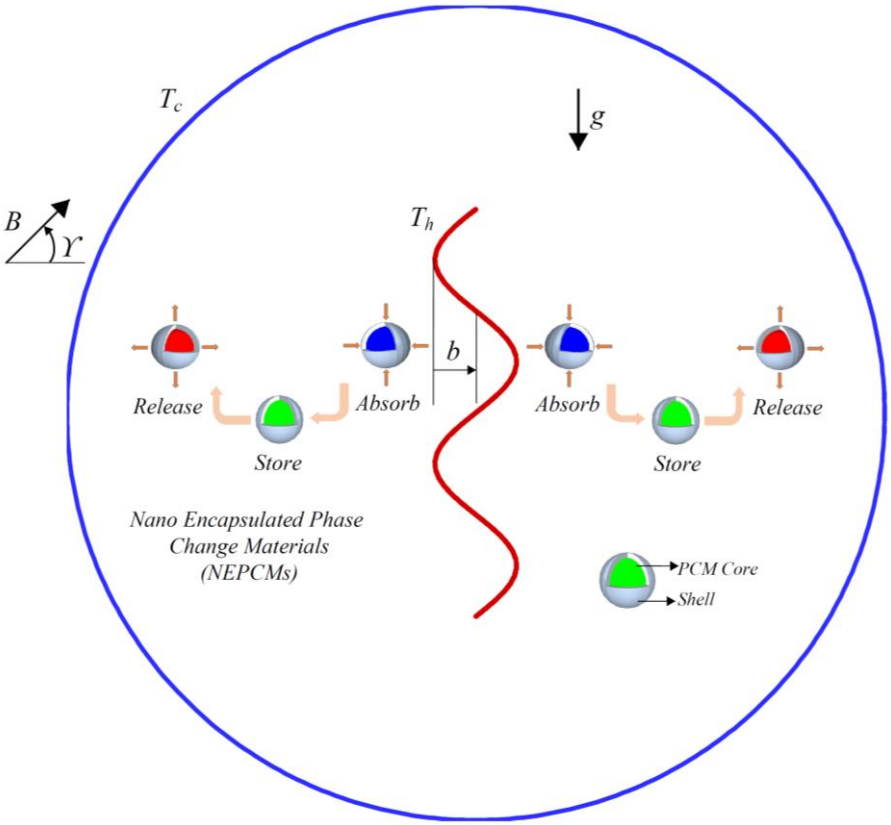

Fig. 1. The geometry of this work

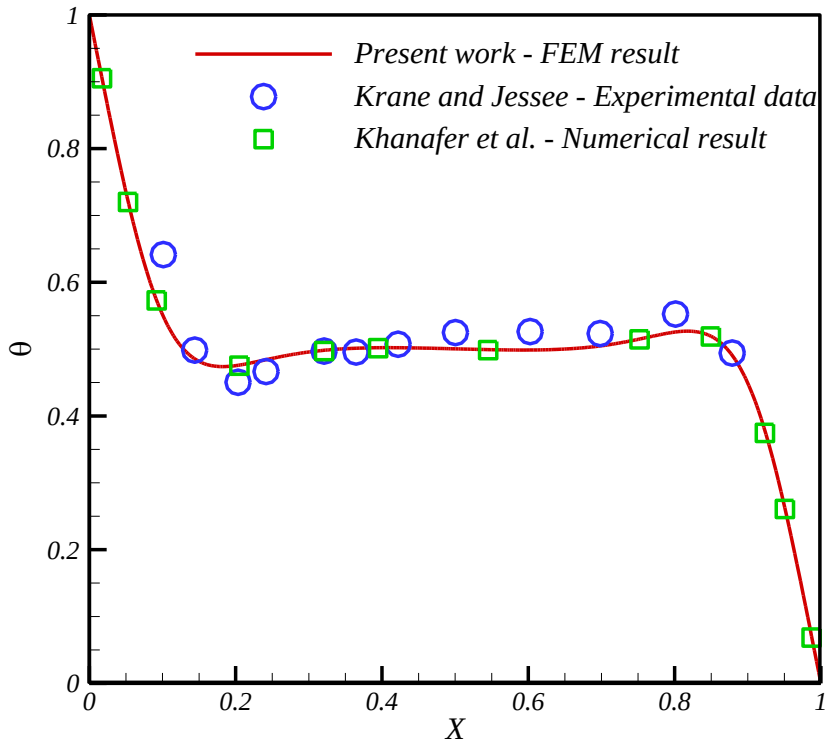

Fig. 2. Experimental [39] and numerical results [40] versus the outcomes of this work

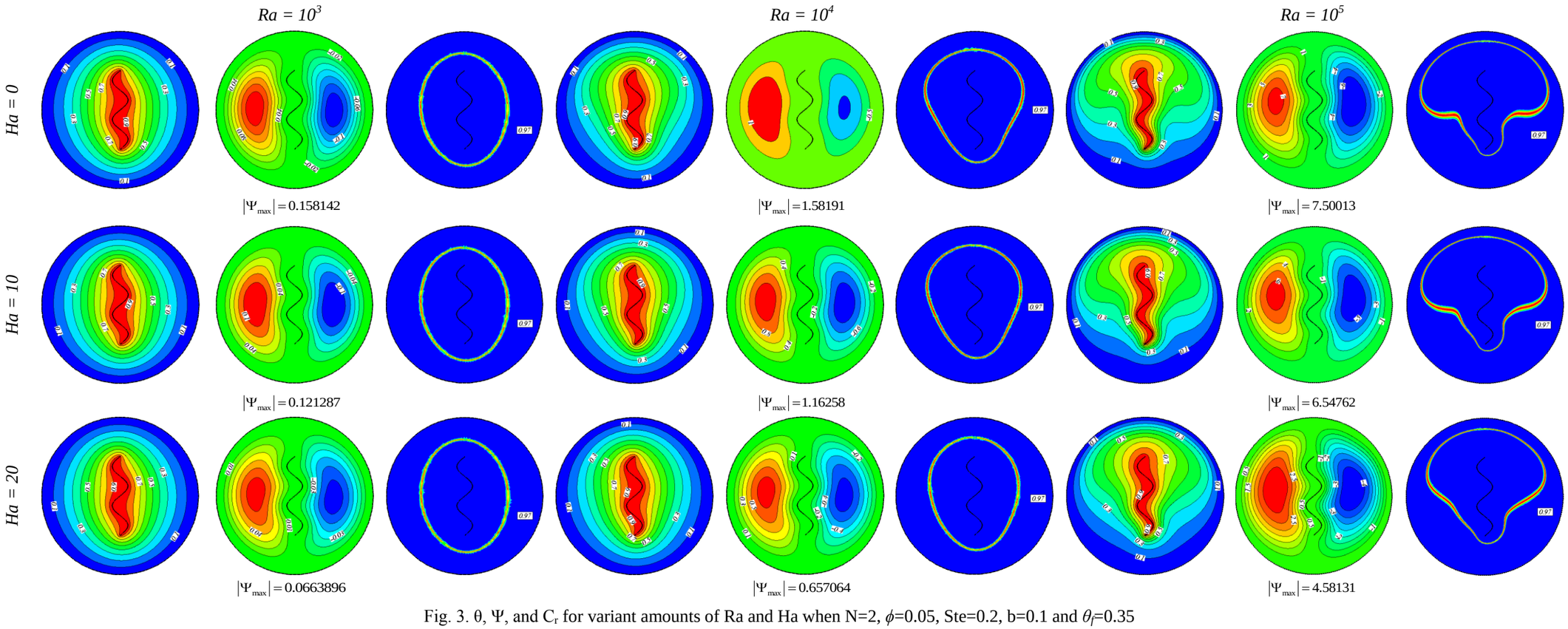

Fig. 3. θ, Ψ, and C_r for variant amounts of Ra and Ha when N=2, ϕ=0.05, Ste=0.2, b=0.1 and θ_f=0.35

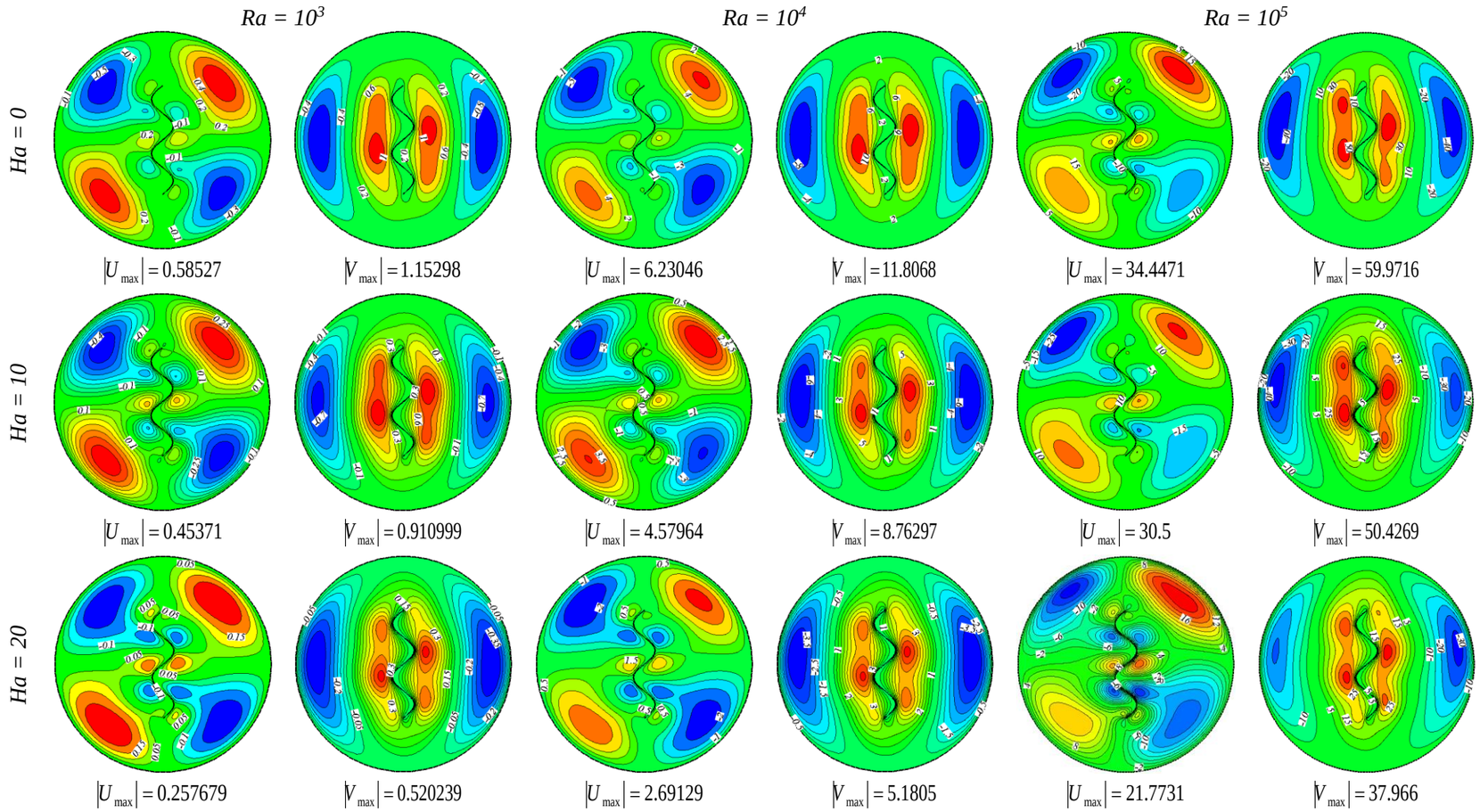

Fig. 4. U and V for variant amounts of Ra and Ha when N=2, ϕ=0.05, Ste=0.2, b=0.1 and θ_f=0.35

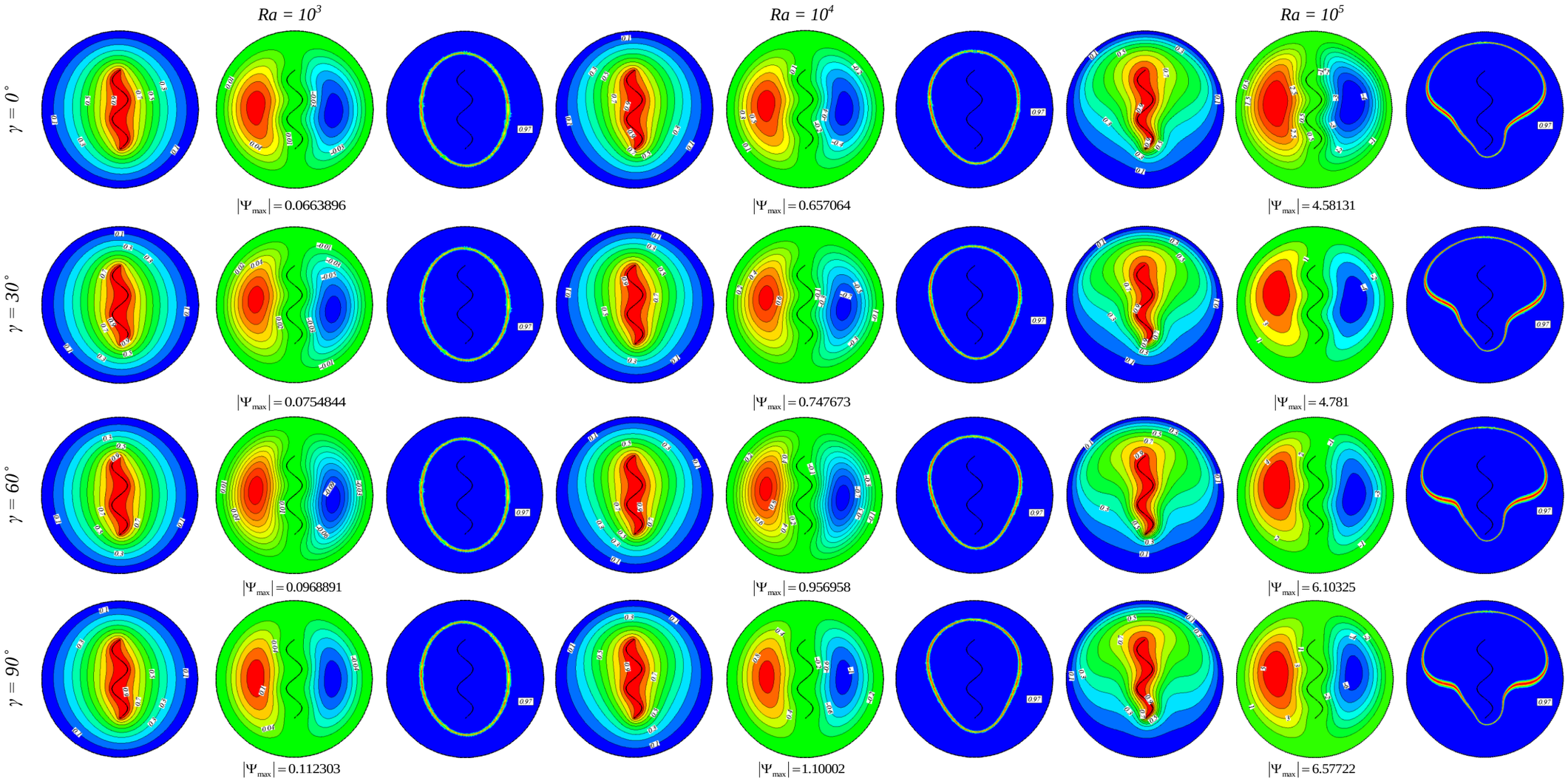

Fig. 5. θ, Ψ, and C_r for variant amounts of γ at diverse *Ra* when N=2, ϕ=0.05, Ste=0.2, b=0.1, Ha=20, and θ_f=0.35

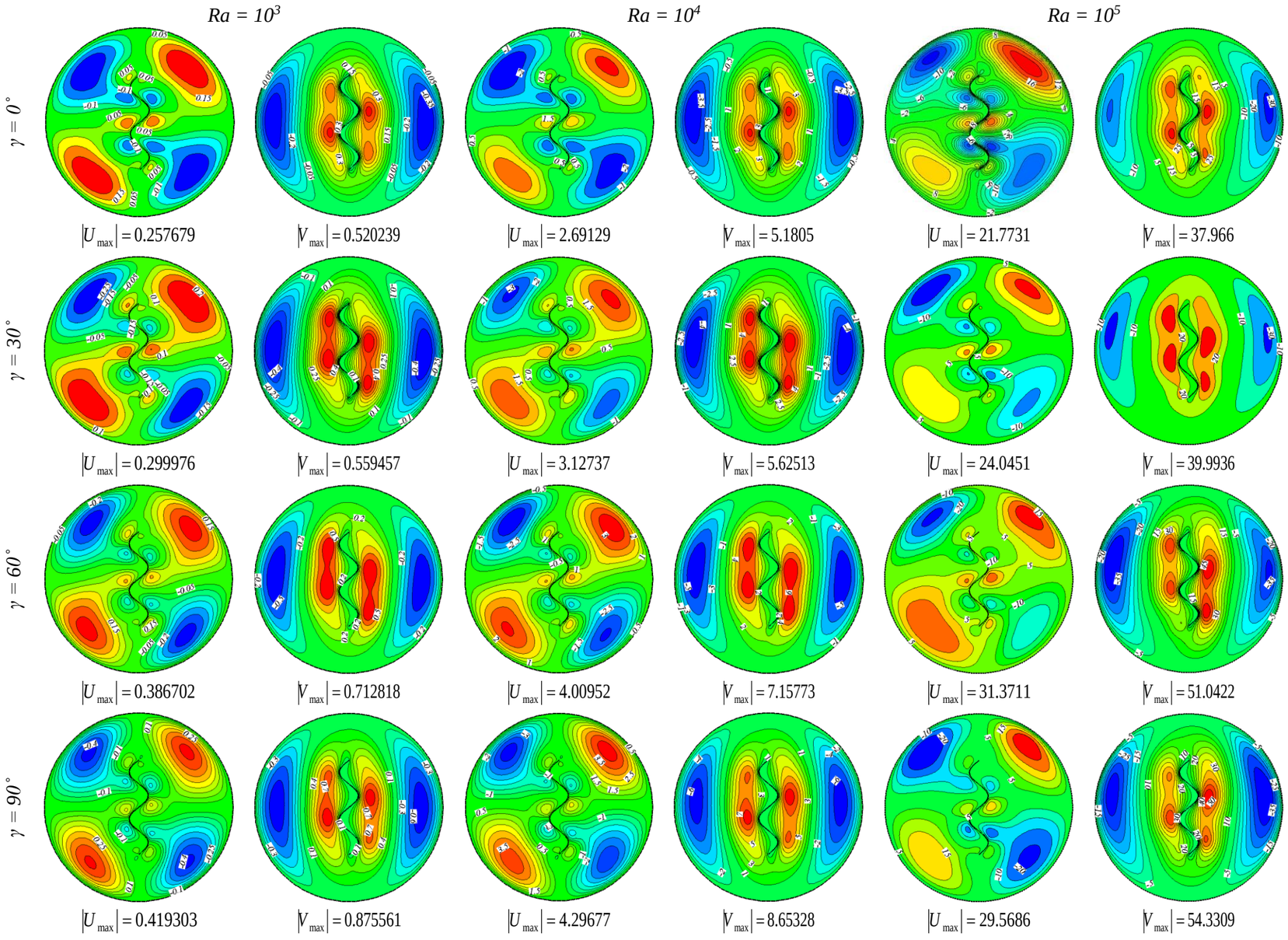

Fig. 6. U and V for variant amounts of γ at diverse *Ra* when N=2, ϕ=0.05, Ste=0.2, b=0.1, Ha=20, and θ_f=0.35

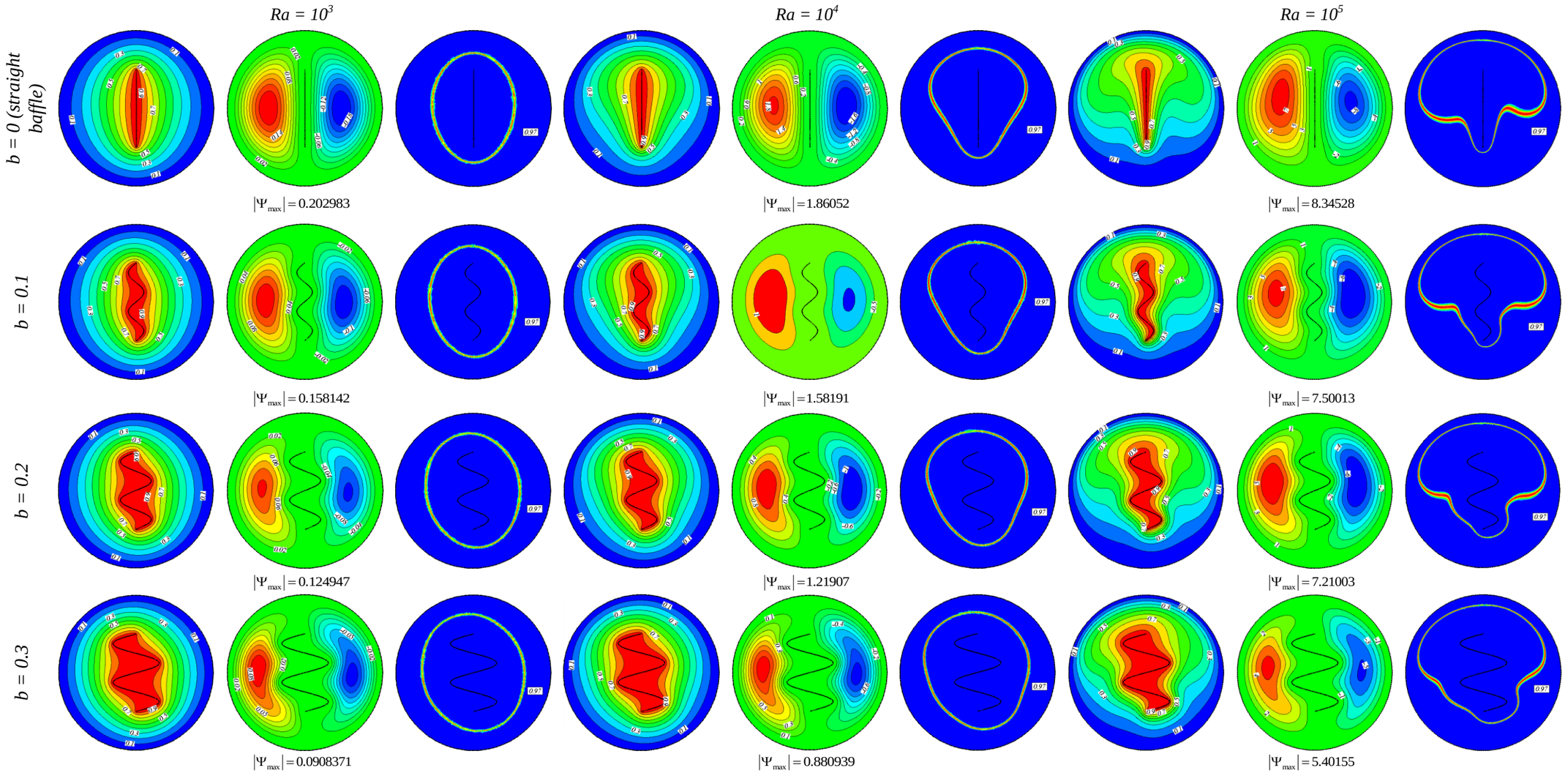

Fig. 7. θ, Ψ, and C_r for variant amounts of Ra and Ha when N=2, ϕ=0.05, Ste=0.2, Ha=0 and θ_f=0.35

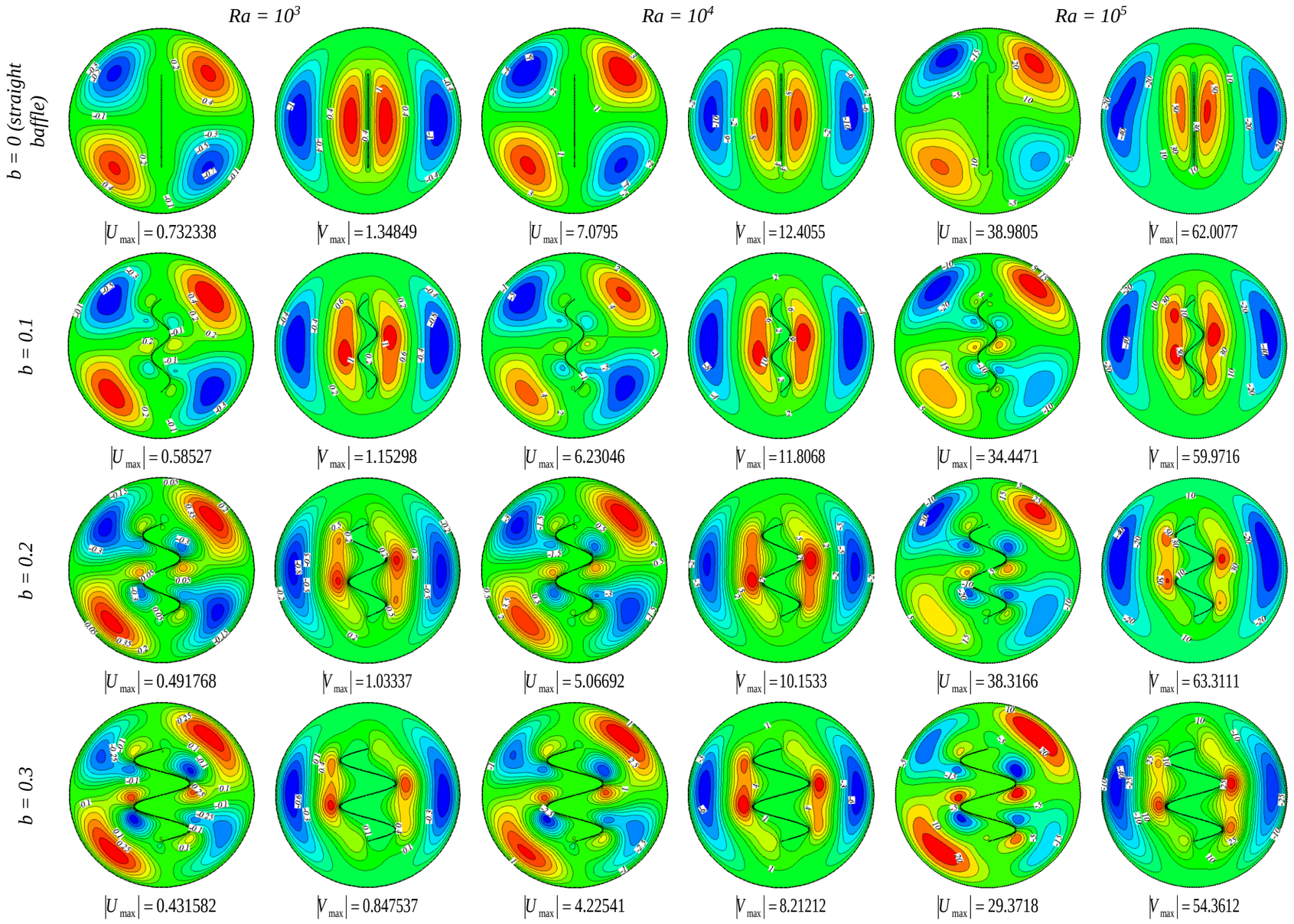

Fig. 8. U and V for variant amounts of γ at diverse *Ra* when N=2, ϕ=0.05, Ste=0.2, Ha=0, and θ_f=0.35

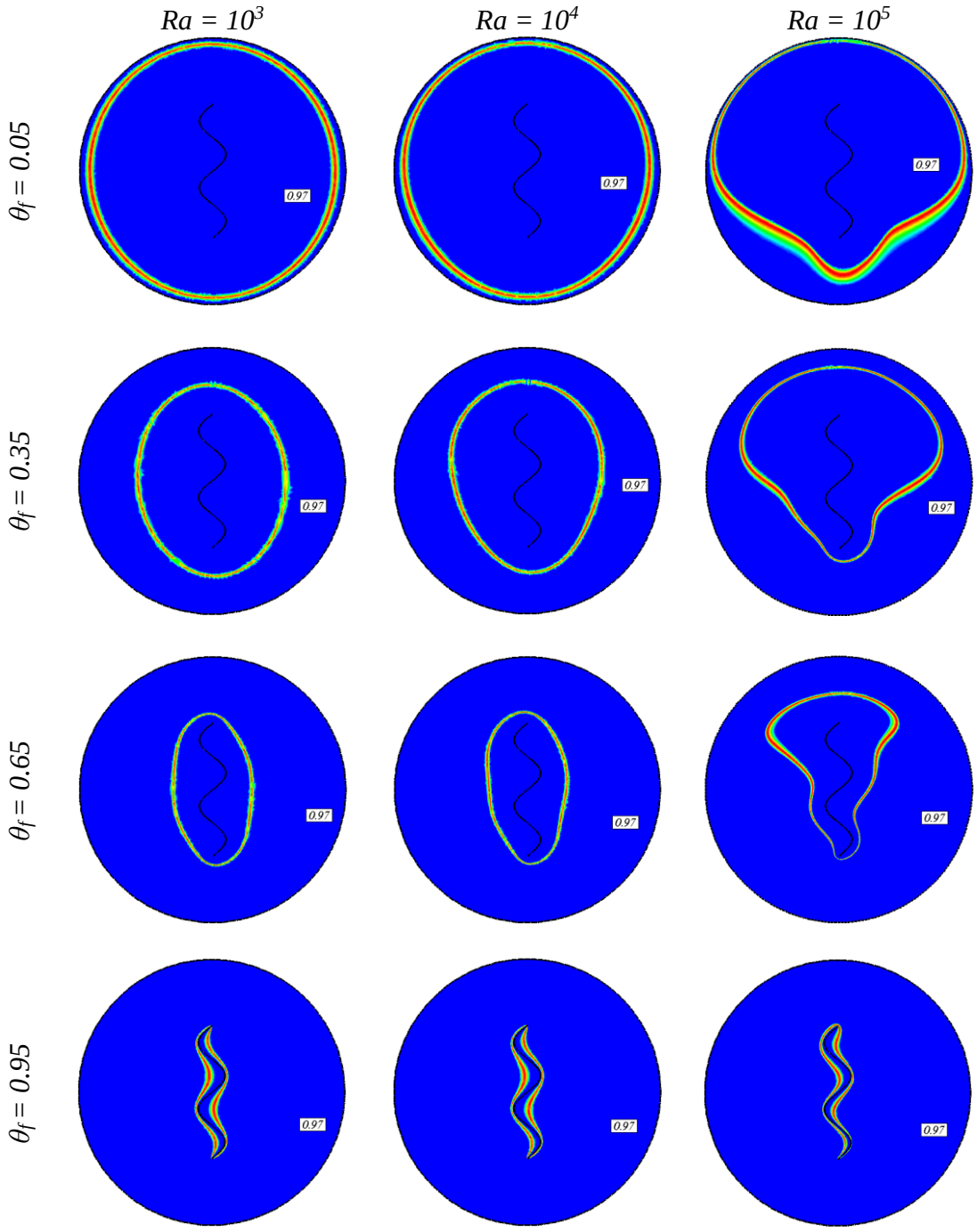

Fig. 9. C_r for variant amounts of θ_f at disparate *Ra* when N=2, ϕ=0.05, Ste=0.2, b=0.1, and Ha=20

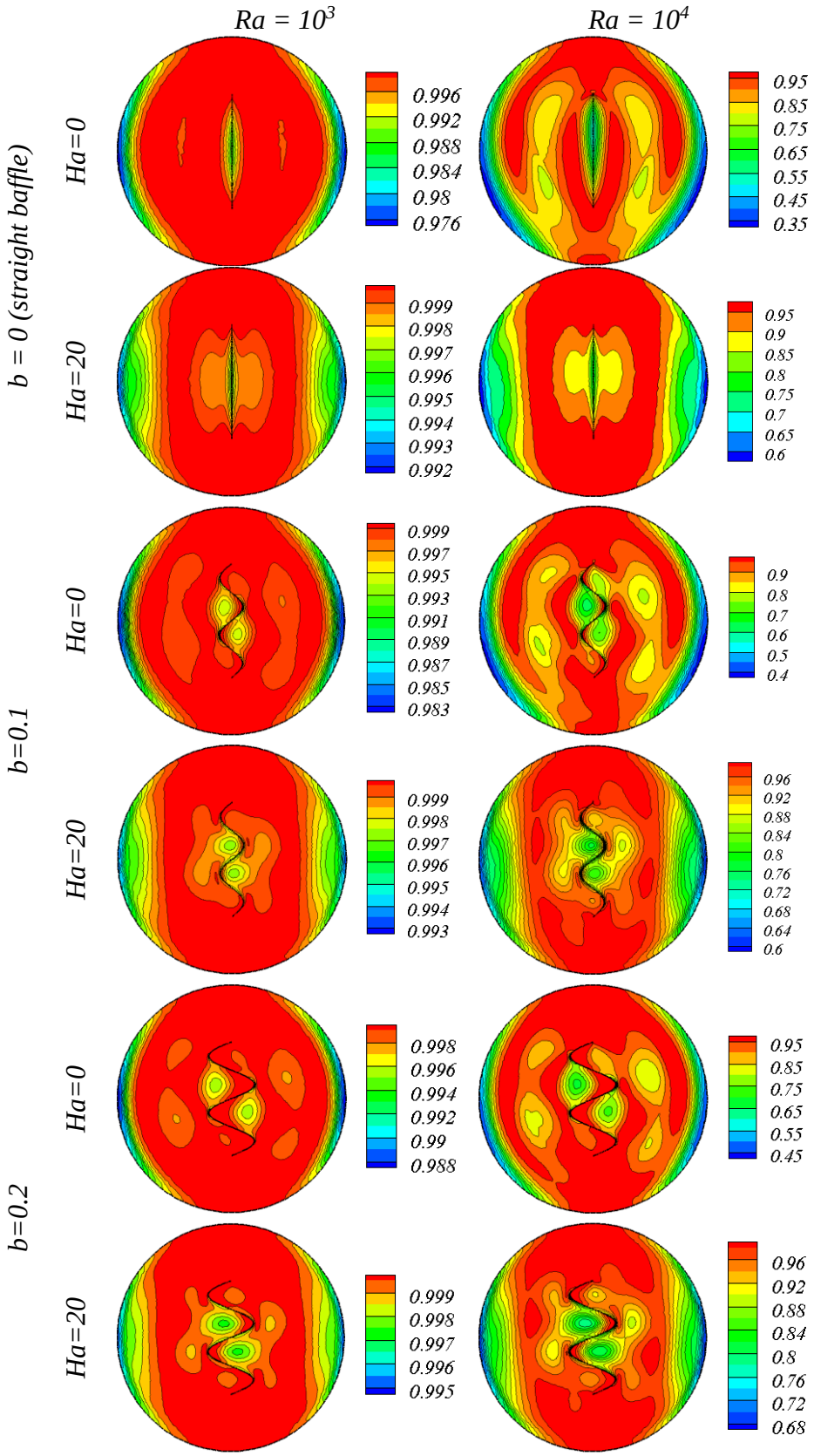

Fig. 10. Be_{loc} for variant amounts of AR, Ha, and Ra

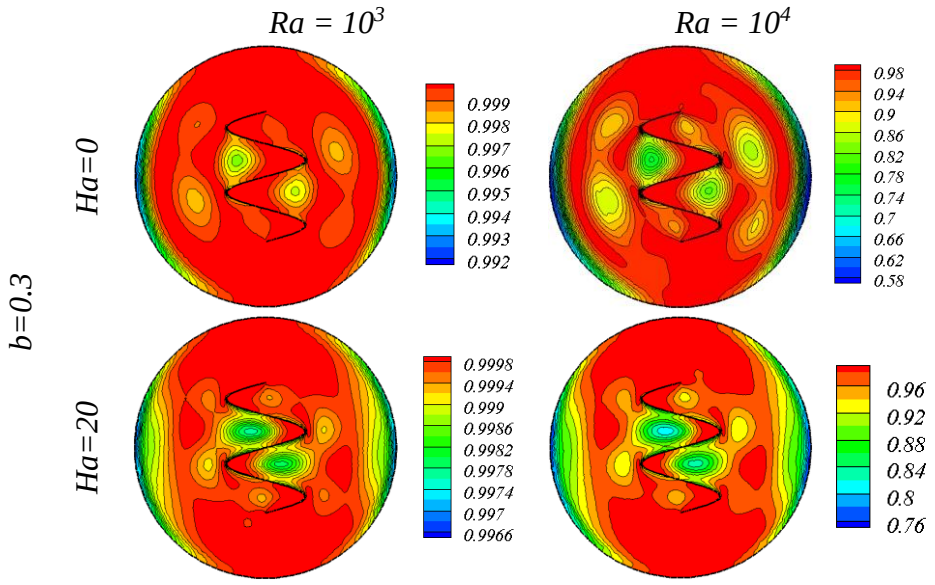

Fig. 10. Continued

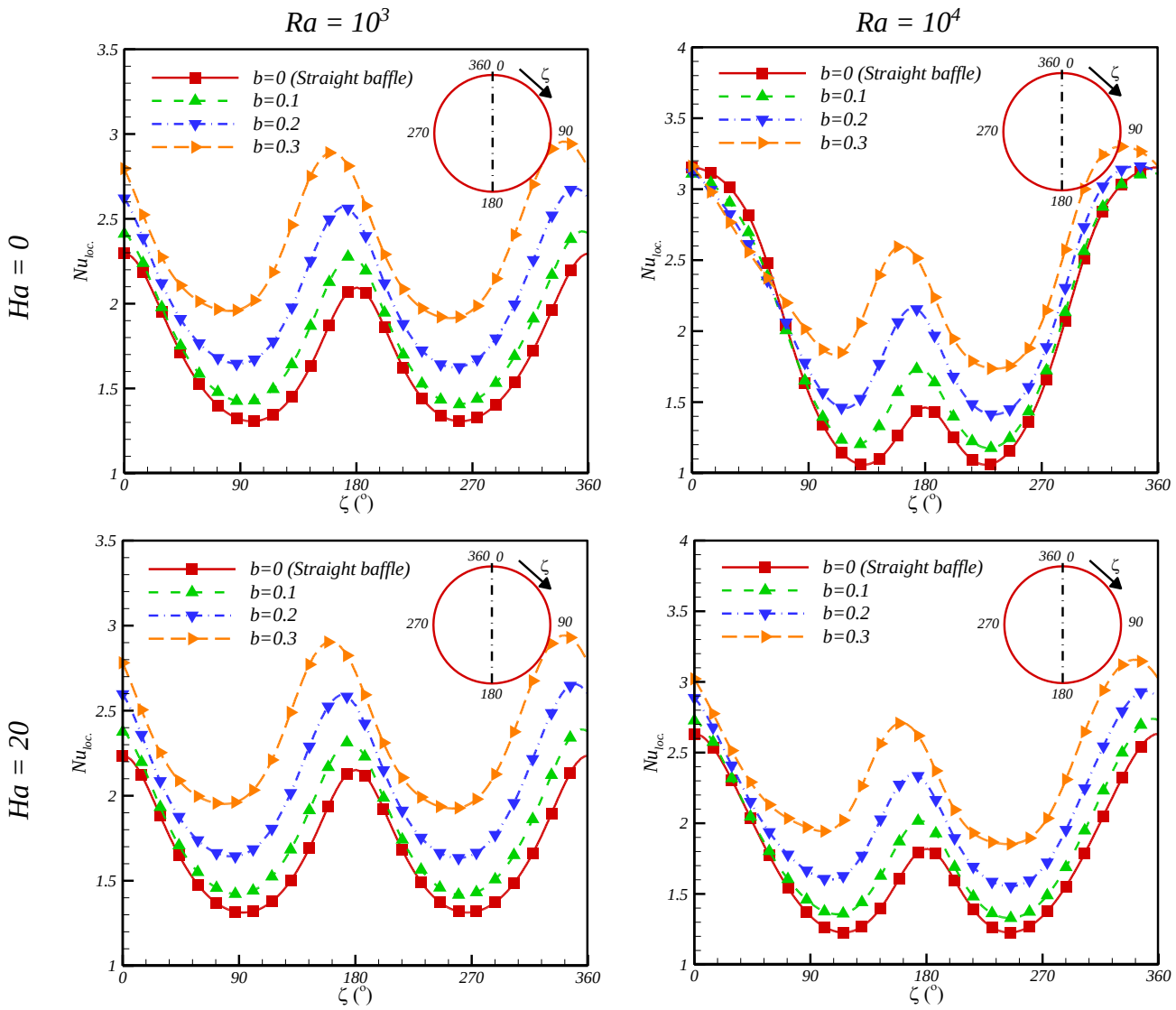

Fig. 11. Nu_{loc} for variant amounts of Ra, b, and Ha

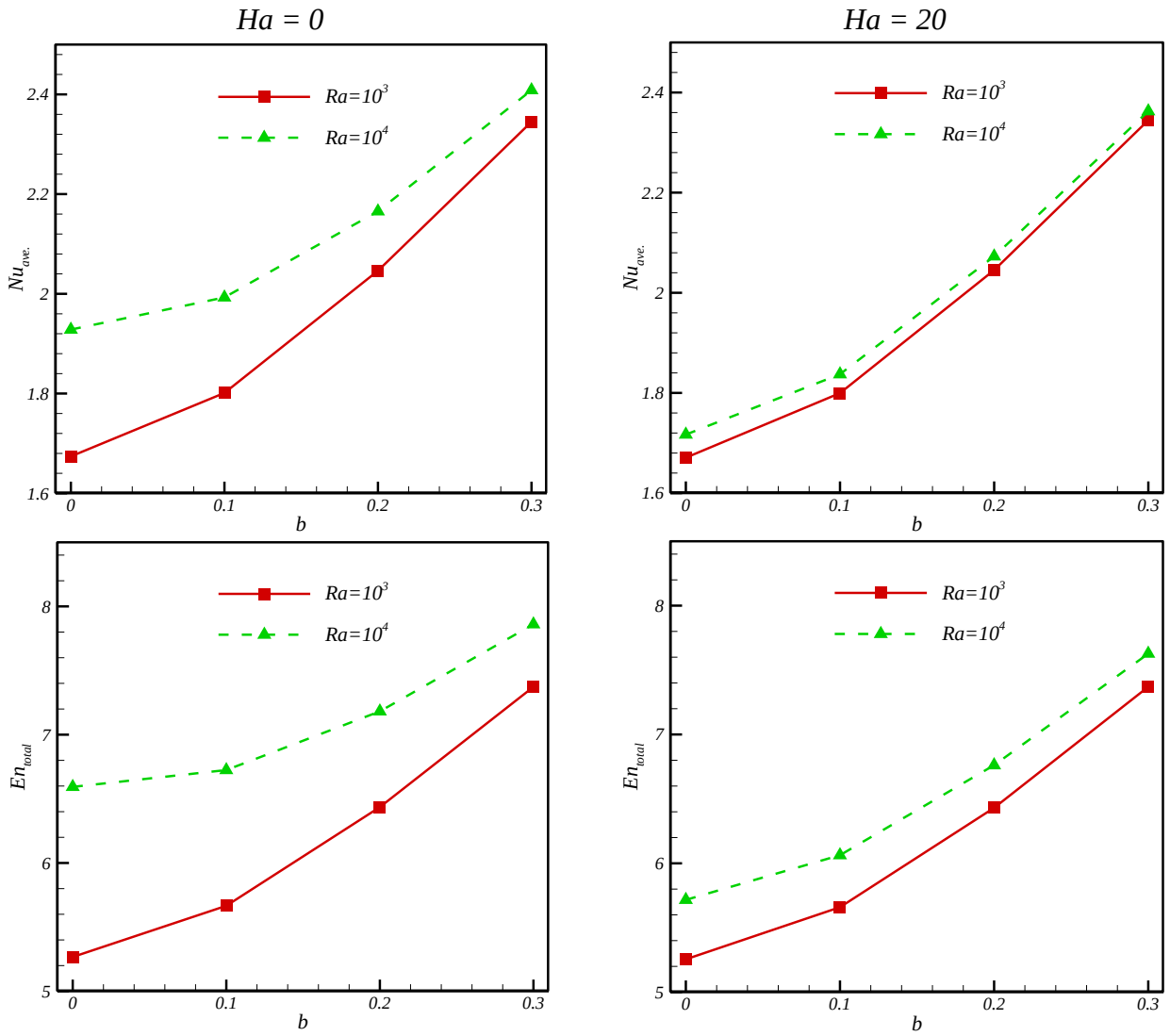

Fig. 12. $Nu_{ave.}$ and En_{total} for variant amounts of Da, Hs and Ra

Table 1. ϕ's impact on $Nu_{ave.}$

Ra	*Ha*	$\phi(\%)$	$Nu_{ave.}$
10^4	0	1	1.7437
		3	1.8711
		5	1.9928
	20	1	1.6386
		3	1.7378
		5	1.8374
10^5	0	1	3.1328
		3	3.5849
		5	3.8681
	20	1	2.5778
		3	2.8641
		5	2.9992

Table 2. η's impact on $Nu_{ave.}$

Ra	η	$Nu_{ave.}$
10^3	0	1.7996
	0.01	1.7991
	0.02	1.7987
10^4	0	1.8374
	0.01	1.7937
	0.02	1.7364

References

[1] Su W, Darkwa J, Kokogiannakis G. Review of solid–liquid phase change materials and their encapsulation technologies. Renew. Sustain. Energy Rev. 2015;48:373-91.

[2] Pielichowska K, Pielichowski K. Phase change materials for thermal energy storage. Prog. Mater Sci. 2014;65:67-123.

[3] Keshteli AN, Sheikholeslami M. Nanoparticle enhanced PCM applications for intensification of thermal performance in building: a review. J. Mol. Liq. 2019;274:516-33

[4] Huang X, Alva G, Jia Y, Fang G. Morphological characterization and applications of phase change materials in thermal energy storage: a review. Renew. Sustain. Energy Rev. 2017;72:128-45.

[5] Sheikholeslami M. Numerical modeling of nano enhanced PCM solidification in an enclosure with metallic fin. J. Mol. Liq. 2018;259:424-38.

[6] Hossain R, Mahmud S, Dutta A, Pop I. Energy storage system based on nanoparticle-enhanced phase change material inside porous medium. Int. J.Therm. Sci. 2015;91:49-58.

[7] Ghalambaz M, Doostani A, Izadpanahi E, Chamkha AJ. Phase-change heat transfer in a cavity heated from below: The effect of utilizing single or hybrid nanoparticles as additives. J. Taiwan Inst. Chem. Eng. 2017;72:104-15.

[8] Hosseini SR, Sheikholeslami M, Ghasemian M, Ganji DD. Nanofluid heat transfer analysis in a microchannel heat sink (MCHS) under the effect of magnetic field by means of KKL model. Powder Technol. 2018;324:36-47.

[9] Sheikholeslami M, Sadoughi MK. Simulation of CuO-water nanofluid heat transfer enhancement in presence of melting surface. Int. J. Heat Mass Transf. 2018;116:909-19.

[10] Elbahjaoui R, El Qarnia H. Transient behavior analysis of the melting of nanoparticle-enhanced phase change material inside a rectangular latent heat storage unit. Appl. Therm. Eng. 2017;112:720-38.

[11] Moukalled F, S. Acharya S. Natural convection in the annulus between concentric horizontal circular and square cylinders. J. Thermophys. Heat Transfer 1996;10:524-31.

[12] Ghaddar NK. Natural convection heat transfer between a uniformly heated cylindrical element and its rectangular enclosure. Int. J. Heat Mass Transfer 1992;35:2327-34.

[13] Kumar De A, Dalal A. A numerical study of natural convection around a square, horizontal, heated cylinder placed in an enclosure. Int. J. Heat Mass Transfer 2006;49: 4608-23.

[14] Kim BS, Lee DS, Ha MY, Yoon HS. A numerical study of natural convection in a square enclosure with a circular cylinder at different vertical locations. Int. J. Heat Mass Transfer 2008;51:1888-906.

[15] Yoon HS, Ha MY, Kim BS, Yu DH. Effect of the position of a circular cylinder in a square enclosure on natural convection at Rayleigh number of 10^7. Phys. Fluids 2009;21:1-11.

[16] Lee JM, Ha MY, Yoon HS. Natural convection in a square enclosure with a circular cylinder at different horizontal and diagonal locations. Int. J. Heat Mass Transfer 2010;53:5905-19.

[17] Li Z, Hussein AK, Younis O, Afrand M, Feng S. Natural convection and entropy generation of a nanofluid around a circular baffle inside an inclined square cavity under thermal radiation and magnetic field effects. Int. Comm. Heat Mass Transf. 2020;116:104650.

[18] Bejan A. Entropy Generation through Heat and Fluid Flow. Wiley 1982.

[19] Bejan A. Second law analysis in heat transfer. Energy 1980;5:720-32.

[20] Oztop HF, Al-Salem K. A review on entropy generation in natural and mixed convection heat transfer for energy systems. Renewable Sustainable Energy Rev. 2012;16:911-20.

[21] Oztop HF, Kolsi L, Alghamdi A, Abu-Hamdeh N, Aissia HB. Numerical analysis of entropy generation due to natural convection in three-dimensional partially open enclosures. J. Taiwan Inst. Chem. Eng. 2017;75:131-40.

[22] Selimefendigil F, Oztop HF, Chamkha AJ. MHD mixed convection and entropy generation of nanofluid filled lid driven cavity under the influence of inclined magnetic fields imposed to its upper and lower diagonal triangular domains. J. Magn. Magn. Mater. 2016;406:266-81.

[23] Fourier JBJ. Theorie Analytique De La Chaleur, Paris 1822.

[24] Christov CI, On frame indifferent formulation of the Maxwell-Cattaneo model of finite-speed heat conduction. Mech. Res. Commun. 2009;36:481-86.

[25] Cattaneo C. Sulla conduzionedelcalore. AttiSemin. Mat. Fis. Univ. Modena Reggio Emilia 1948;3:83-101.

[26] Waqas M, Hayat T, Farooq M, Shehzad SA, Alsaedi A. Cattaneo-Christov heat flux model for flow of variable thermal conductivity generalized burgers fluid. J.Mol. Liq. 2016;220:642-8.

[27] Waqas M, Hayat T, Shehzad SA, Alsaedi A. Application of improved Fourier's and Fick's laws in a non-Newtonian fluid with temperature-dependent thermal conductivity. J. Braz. Soc. Mech. Sci. Eng. 2018;40:116.

[28] Dogonchi AS, Ganji DD. Impact of Cattaneo-Christov heat flux on MHD nanofluid flow and heat transfer between parallel plates considering thermal radiation effect. J. Taiwan Inst. Chem. Eng. 2017;80:52-63.

[29] Sheikholeslami M. Numerical approach for MHD Al2O3-water nanofluid transportation inside a permeable medium using innovative computer method. Comput Methods Appl Mech Eng. 2019;344:306-18.

[30] Sathiyamoorthy M, Chamkha AJ. Effect of magnetic field on natural convection flow in a liquid gallium filled square cavity for linearly heated side wall(s). Int. J. Therm. Sci. 2010;49:1856-65.

[31] Sivasankaran S, Malleswaran A, Lee J, Sundar P. Hydro-magnetic combined convection in a lid-driven cavity with sinusoidal boundary conditions on both sidewalls. Int. J. Heat Mass Transfer 2011;54:512-25.

[32] Oztop HF, Al-Salem K, Pop I. MHD mixed convection in a lid-driven cavity with corner heater. Int. J. Heat Mass Transfer 2011;54:3494-504.

[33] Ashorynejad HR, Mohamad AA, Sheikholeslami M. Magnetic field effects on natural convection flow of a nanofluid in a horizontal cylindrical annulus using Lattice Boltzmann method. Int. J. Therm. Sci. 2013;64:240-50.

[34] Ghalambaz M, Doostanidezfuli A, Zargartalebi H, Chamkha AJ. MHD phase change heat transfer in an inclined enclosure: Effect of a magnetic field and cavity inclination. Num. Heat Transfer Part A: Appl. 2017;71:91-109.

[35] Selimefendigil F, Oztop HF. Conjugate natural convection in a nanofluid filled partitioned horizontal annulus formed by two isothermal cylinder surfaces under magnetic field. Int. J. Heat Mass Transf. 2017;108:156-71.

[36] Geridonmez BP, Oztop HF, Natural convection in a cavity under partial magnetic field applied from different corners. Int. Com Heat Mass Trans 2020;114:104575.

[37] Li Z, Hussein AK, Younis O, Afrand M, Feng S. Natural convection and entropy generation of a nanofluid around a circular baffle inside an inclined square cavity under

thermal radiation and magnetic field effects. Int. Com. Heat Mass Trans 2020;116:104650.

[38] Ghalambaz M, Chamkha AJ, Wen D. Natural convective flow and heat transfer of Nano-Encapsulated Phase Change Materials (NEPCMs) in a cavity. Int. J. Heat Mass Transfer 2019;138:738-49.

[39] Krane RJ, Jessee J. Some detailed field measurements for a natural convection flow in a vertical square enclosure. Proc. of the First ASME-JSME Therm. Eng. Joint Conf. 1983;1:323-29.

[40] Khanafer K, Vafai K, Lightstone M. Buoyancy-driven heat transfer enhancement in a two-dimensional enclosure utilizing nanofluids. Int. J. Heat Mass Transfer 2003;46:3639-53.

Graphical Abstract:

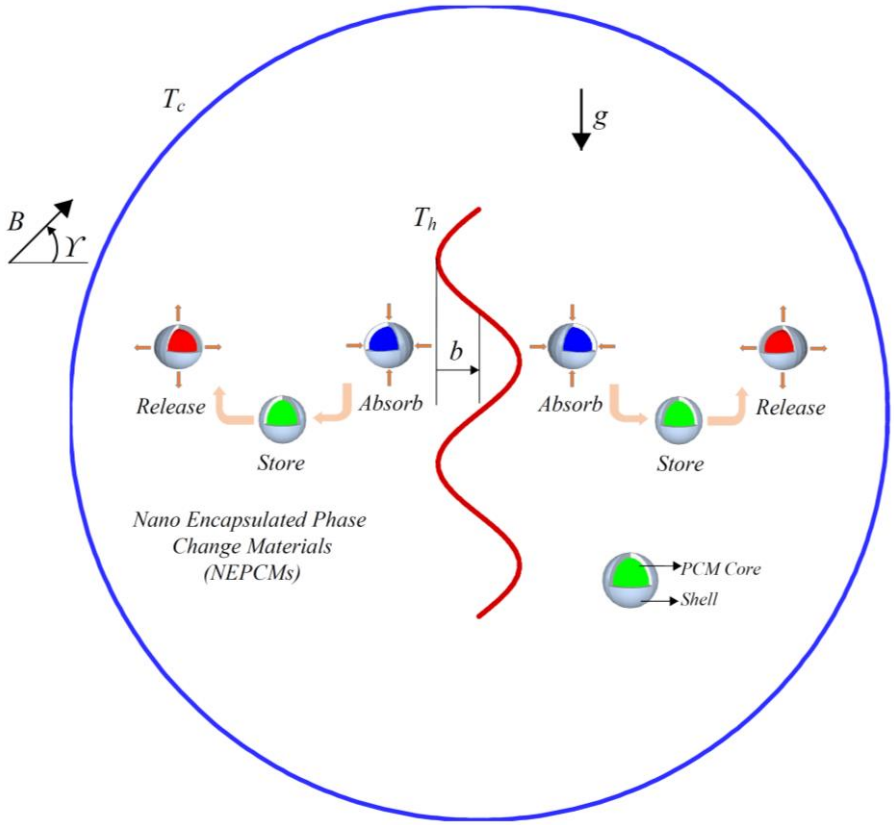

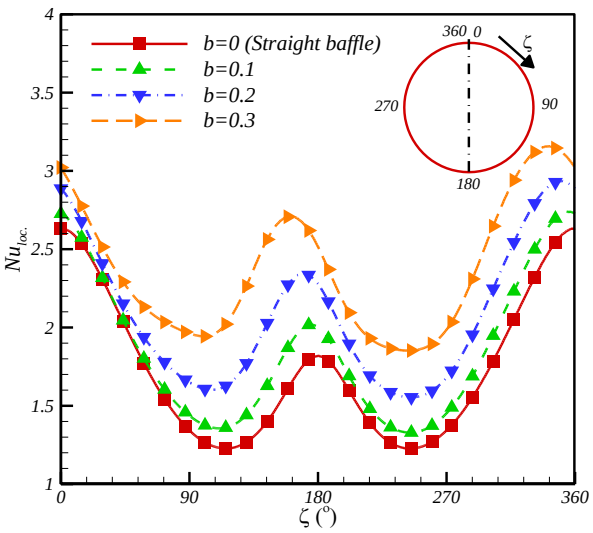

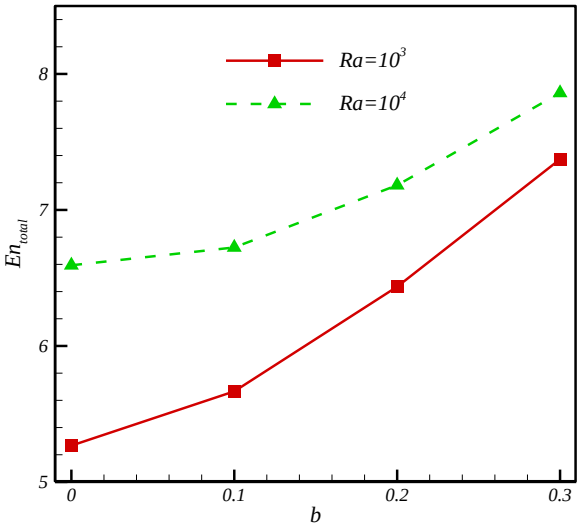

Declaration of interests

☒ The authors declare that they have no known competing financial interests or personal relationships that could have appeared to influence the work reported in this paper.

☐The authors declare the following financial interests/personal relationships which may be considered as potential competing interests:
